



# The distribution, concentration, and toxicity of enhanced green fluorescent protein in retinal cells after genomic or somatic (virus-mediated) gene transfer

Tonia S. Rex,<sup>1</sup> John A. Peet,<sup>1</sup> Enrico M. Surace,<sup>2</sup> Peter D. Calvert,<sup>1</sup> Sergei S. Nikonov,<sup>1</sup> Arkady L. Lyubarsky,<sup>1</sup> Elisabeth Bendo,<sup>1</sup> Thomas Hughes,<sup>3</sup> E. N. Pugh Jr.,<sup>1</sup> Jean Bennett<sup>1</sup>

<sup>1</sup>F. M. Kirby Center for Molecular Ophthalmology, University of Pennsylvania, Philadelphia, PA; <sup>2</sup>Telethon Institute of Genetics and Medicine (TIGEM), Napoli, Italy; <sup>3</sup>Department of Cell Biology & Neuroscience, Montana State University, Bozeman, MT

**Purpose:** The concentration of enhanced green fluorescent protein (EGFP) in individual photoreceptor cells of live mouse retina was quantified and correlated with physiological measurements of cell function.

**Methods:** EGFP protein levels in the retinas of mice injected subretinally by either one of two serotypes of adeno-associated virus (AAV; AAV2/5.CMV.EGFP; AAV2/2.CMV.EGFP) were quantified with a photon-counting confocal laser scanning microscope and compared with those of transgenic mice whose retinas expressed *EGFP* under the  $\beta$ -actin (p $\beta$ Act) or human L/M-cone opsin (pLMCOps) promoter. Single-cell suction pipette recordings of single rods and whole-field electroretinograms (ERGs) were performed to assess retinal cell function.

**Results:** The highest levels of EGFP (680  $\mu$ M) were in the retinal pigment epithelium (RPE) cells of the AAV-transduced eyes. Living photoreceptors of p $\beta$ Act.EGFP mice contained 270  $\mu$ M EGFP, while their bipolars had 440  $\mu$ M. The cones of pLMCOps.EGFP mice expressed 60  $\mu$ M protein. The amplitudes of the major components of ERGs were within the normal range for all transgenic animals examined, and single cell recordings from living p $\beta$ Act.EGFP rods were indistinguishable from those of controls.

**Conclusions:** EGFP levels in individual cells of live mouse retinas can be quantified, so that the efficacy of gene transfer methods can be quantified. Concentrations of several hundred  $\mu$ M are not deleterious to normal function of photoreceptors and bipolar cells. This approach can also be used to quantify levels of biologically active EGFP fusion proteins.

Enhanced green fluorescent protein (EGFP) is widely used in biomedical research to identify the tissues and cells in which specific promoters are active [1,2] and to determine which cells can be targeted by different vectors in viral mediated gene transfer [3-6]. The successful restoration of visual function in animals with defective RPE65 by viral mediated gene transfer [7-10] has raised the possibility that defects of many retinally expressed genes could be similarly treated. However, as normal function depends on the presence of each protein in the appropriate concentration, it will be increasingly important to have means of quantifying the efficiency of transduction of different vectors. *EGFP* expression could provide a means of assessing different vectors and gene delivery methods, but questions have been raised about its potential toxicity.

Recent studies have addressed the question of EGFP toxicity in the retina [11-15]. The studies reported no evidence of toxicity of *EGFP* expression in retinas, but none quantified the concentrations of EGFP in specific cells. Thus, in this investigation we have undertaken to quantify EGFP levels in different retinal cell types in mice carrying the *EGFP* transgene

either by genomic or somatic (virus-mediated) gene transfer, and to assess the physiological function of key cell types in which *EGFP* is expressed. We have also quantified EGFP levels in retinal cells transduced with two different recombinant adeno-associated virus (AAV) serotypes (AAV2/2 and AAV2/5) in utero. This expands upon previous qualitative studies which focused on adult retina as a target [6,16,17].

## METHODS

**Animals:** All experiments were performed in compliance with National Institutes of Health and institutional guidelines. All mice were on a C57Bl/6 background. Transgenic mice expressing *EGFP* driven from the  $\beta$ -actin promoter (p $\beta$ Act.EGFP mice) were purchased from Jackson Laboratories (Bar Harbor, ME). Mice in which *EGFP* is expressed under control of the human long/medium wavelength cone opsin promoter (pLMCOps.EGFP mice) were created previously [18]. Animals were born and maintained in controlled ambient illumination on a 12 h light/dark cycle. Results were compared to data from wild-type C57Bl/6 mice.

Subretinal injections of AAV2/2.CMV.EGFP, or AAV2/5.CMV.EGFP were performed in utero at E14 in C57Bl/6 mice [4]; the same volume and virus titer were used for injections of both serotypes to enable comparison of gene transfer efficacy. Use of in utero delivery results in uniform transduction of a large area of the retina [4]. Animals were sacrificed and eyes were processed on P30.

Correspondence to: Dr. Jean Bennett, F. M. Kirby Center for Molecular Ophthalmology, University of Pennsylvania, 310 Stellar-Chance Laboratories, 422 Curie Boulevard, Philadelphia, PA, 19104; Phone: (215) 898-0915; FAX: (215) 573-7155; email: jebennet@mail.med.upenn.edu

**Electroretinogram (ERG) measurements:** Whole eye electrical activity measurements were performed as described by Lyubarsky et al. [19,20]. Briefly, 12 h dark-adapted mice were anesthetized with an intraperitoneal injection of ketamine/xylazine/urethane (25/10/1000  $\mu\text{g}$  per g body weight) and placed onto a warmed (37 °C) platform. The eyes were dilated with 1% Mydracil (Alcon, Fort Worth, TX). Full-field ERGs were recorded from both eyes using differential amplifiers with a bandwidth of 0.1 Hz to 1 kHz. The filtered traces were digitized at 5 kHz. Platinum wires embedded in contact lenses served as the corneal electrodes, which were placed on each eye. The reference electrode was in the animal's mouth. The recording chamber served as both a Faraday cage and a Ganzfeld, with appropriate ports and baffles to ensure uniform illumination. Intensities were calibrated as previously described.

**Single cell recordings:** Rod recordings were performed according to Nikonov et al. [21]. Briefly, mice were sacrificed, enucleated, and whole neural retinas were isolated from the RPE/choroid under infrared light. Small pieces of neural retina were then placed into the recording chamber. The chamber was filled with Locke's solution (112.5 mM NaCl, 3.6 mM KCl, 2.4 mM MgCl<sub>2</sub>, 1.2 mM CaCl<sub>2</sub>, 10 mM Hepes, 0.02 mM EDTA, 20 mM NaHCO<sub>3</sub>, 3 mM Na<sub>2</sub>-succinate, 0.5 mM Na-glutamate, 10 mM glucose, pH 7.4, 300 mOsm) bubbled

with 95% O<sub>2</sub>/5% CO<sub>2</sub> and maintained at 37 °C during the procedure. A single piece of retina was placed into a chamber under the microscope. For recording, an individual rod outer segment was drawn into a silanized suction recording pipette connected by a salt bridge to a current-to-voltage converter circuit. Electrical responses were evoked with calibrated flashes of light under the control of a customized LabView (National Instruments, Austin, TX) interface. After completion of the electrical recording from a rod, the microscope, operating in epifluorescence mode, was used to confirm the presence of EGFP in the recorded cell.

**Tissue processing:** After ERGs were collected, mice were euthanized by Avertin overdose and enucleated for subsequent assays. For histology, eyes were incubated in cold 4% paraformaldehyde at 4 °C for up to 24 h. Eyes were rinsed with phosphate buffered saline (PBS) and transferred to 30% sucrose in PBS. They were incubated overnight at 4 °C, then embedded in tissue freezing medium (Triangle Biomedical Sciences, NC) and frozen in dry ice and ethanol. Sections 10 to 25  $\mu\text{m}$  thick were collected, placed onto slides and stored at -30 °C.

**Confocal microscopy:** Tissue sections were rinsed in PBS, blocked in normal donkey serum in PBTA (PBS, BSA, Triton X-100, sodium azide) for two h at room temperature, then incubated overnight at 4 °C in 40  $\mu\text{g}/\text{ml}$  biotinylated PNA in

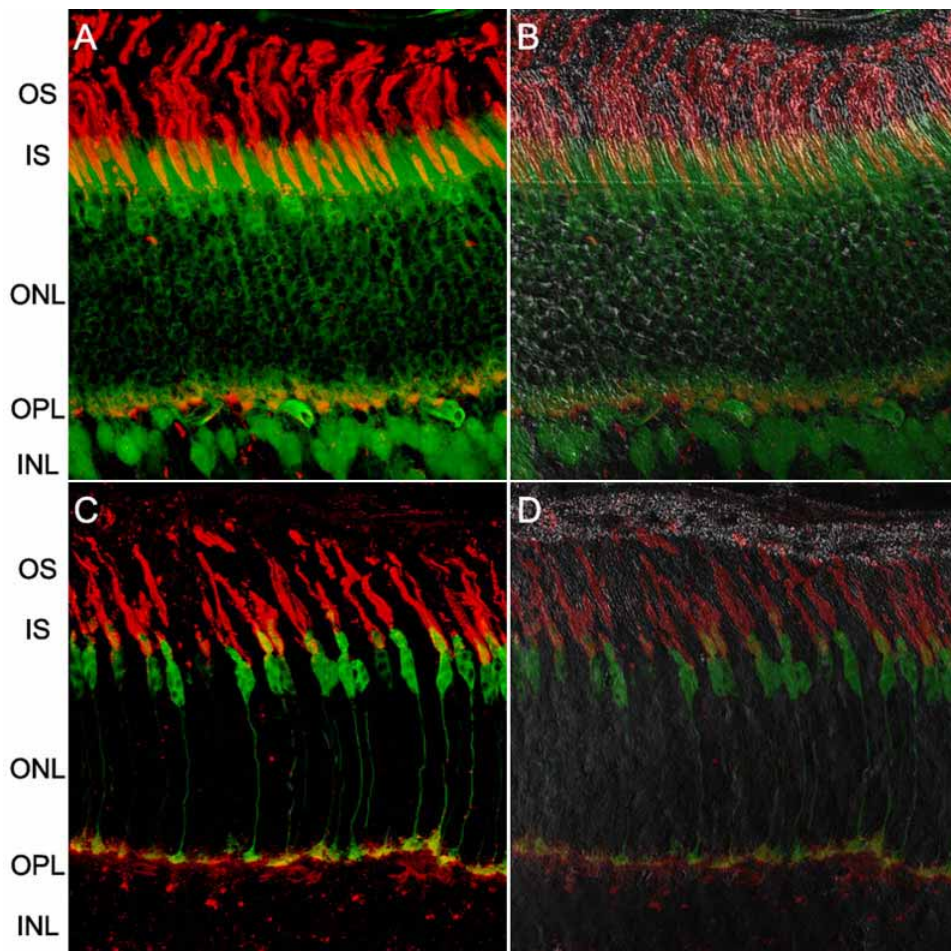


Figure 1. Distribution of enhanced green fluorescent protein in photo-receptors in transgenic mice. The retinal structure of mice expressing enhanced green fluorescent protein (EGFP) under two different promoters—one constitutive and the other cell-specific, is typical of that found normally in a C57Bl/6 wild type (WT) retina. **A,B:** Images of a frozen section of a retina expressing EGFP under control of the  $\beta$ -actin promoter. **C,D:** Images of a section of the retina of a mouse expressing EGFP under control of the human cone L/M opsin promoter. **A,C:** Confocal fluorescence scans with the green channel reporting EGFP fluorescence, while the red channel shows PNA staining, primarily of the cone matrix sheaths. **B,D:** Differential interference contrast (DIC) images overlaid on the corresponding fluorescence sections at left, with the DIC images shown at 65% transparency. The images are each about 100  $\mu\text{m}$  x 100  $\mu\text{m}$ . The outer segment layer (OS), inner segment layer (IS), outer nuclear layer (ONL), and outer plexiform layer (OPL) are identified.

PBTA. The following day, the sections were rinsed in PBS and incubated for 1 h at room temperature in avidin-Cy3. Finally, the sections were rinsed and mounted in Vectashield with DAPI (Vector Labs, Burlingame, CA). Sections were scanned on a Zeiss laser scanning confocal microscope (Zeiss, Germany).

*Quantitative confocal laser scanning microscopy:* The methods used for quantifying EGFP concentrations in living rod cells have been described in Peet et al. [22]. Briefly, known concentrations of recombinant EGFP in solution were scanned with measured laser excitation levels, and fluorescence emission calibration curves were generated. This information was used to convert measured fluorescence into EGFP concentration. In the majority of situations, EGFP concentration was measured in multiple individual cells of each particular cell type. For live retinal scanning, retinas were isolated and small pieces were placed into chambers holding 10  $\mu$ l of Locke's buffer. For all imaging, a 60x water-immersion objective was used. Images of single cells were digitally isolated (in 3D) from images acquired during the confocal scans, and the fluorescence intensity was then converted into EGFP concentration with customized Matlab™ (The Mathworks, Natick, MA) software.

## RESULTS

*Retinal morphology is normal in retinal cells expressing high levels of EGFP:* The morphology of retinal cells was completely normal in the p $\beta$ Act.EGFP mice (Figure 1A,B) [14,23]. In these mice, rods, cones and bipolar cells had high levels of EGFP. Expression in rods (Figure 1A) is confirmed

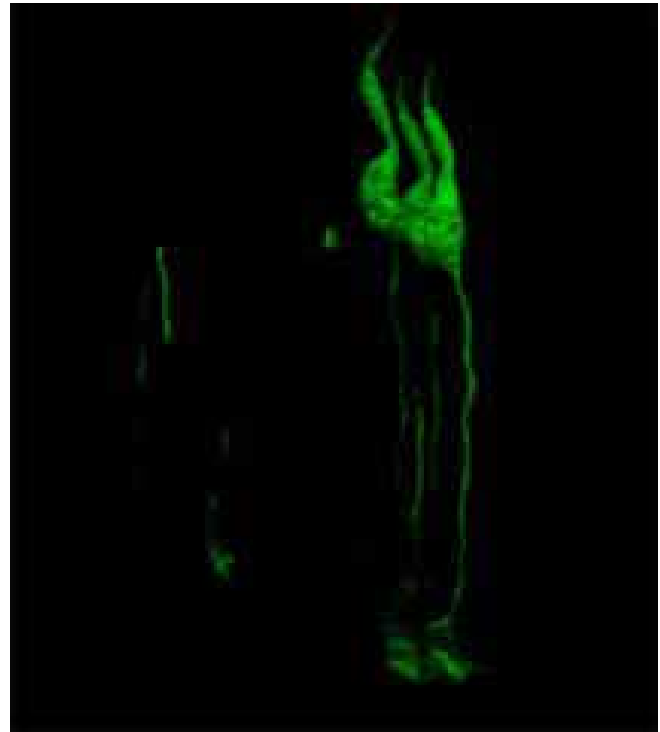


Figure 2. Morphology of a LMCops.EGFP cone photoreceptor. Distribution of enhanced green fluorescent protein in cone photoreceptors of the LMCops. EGFP transgenic mouse. A quicktime movie of this figure is available in the online version of this article. A representative frame is included here.

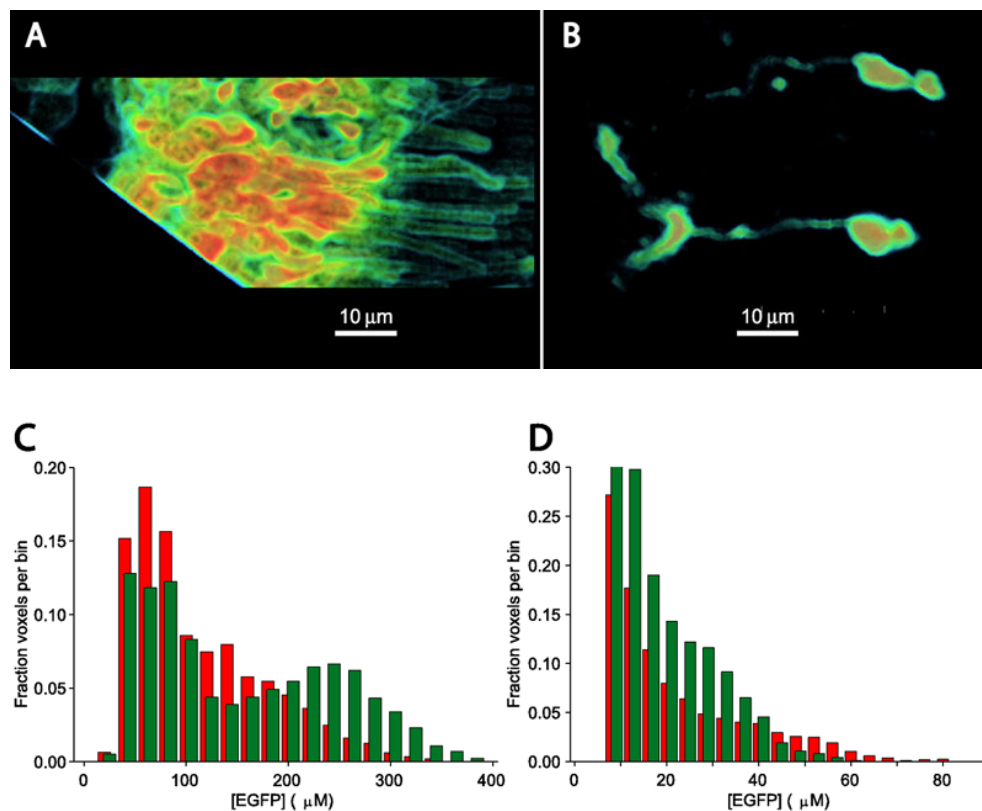


Figure 3. Determination of the concentration of enhanced green fluorescent protein in living photoreceptors. **A:** Confocal fluorescence image of a slice of live retina of mouse expressing EGFP under control of the  $\beta$ -actin promoter. **B:** Confocal image of slice of live retina of mouse expressing EGFP under control of the human L/M cone opsin promoter. The intensities of EGFP fluorescence from the voxels in both images have been mapped onto a pseudocolor scale that ranges from blue (low intensity) to high (red). **C,D:** Histograms of the intensity distributions of the voxels of two rods from **C** and the two cones in **D**; the intensities have been converted to the concentrations of EGFP, as described [22]. The concentrations estimated for the 4 cells are 250  $\mu$ M (red bars in **C**) and 314  $\mu$ M (green bars in **C**), 41  $\mu$ M (green bars in **D**), and 54  $\mu$ M (red bars in **D**).

by strong fluorescence throughout the outer nuclear layer and in particular by the very strong fluorescence in the photoreceptor inner segment layer. This correlates with results from previous work on amphibian and murine rods that led to the expectation of relatively higher concentrations of protein in

the rod inner segment [22,24]. Expression in cones (Figure 1A) is confirmed by staining with the lectin peanut agglutinin (PNA), which binds specifically to the cone matrix sheath [25].

A distinct pattern of EGFP fluorescence is seen in the retinas of pLMHCops.EGFP mice. In these retinas, as reported

**TABLE 1. CONCENTRATIONS OF ENHANCED GREEN FLUORESCENT PROTEIN IN RETINAL CELLS**

Delivery method	Promoter	Cell type	[EGFP] ( $\mu\text{M}$ )	Number cells	Number of retinas analyzed	Fixation effect (fold decrease)
Genomic	$\beta$ -actin	Live rod and cone	270 $\pm$ 12	105	8	-
Genomic	$\beta$ -actin	Fixed rod and cone	120 $\pm$ 19	31	5	2.3
Genomic	$\beta$ -actin	Live bipolar	440 $\pm$ 60	24	4	-
Genomic	$\beta$ -actin	Fixed bipolar	220 $\pm$ 14	5	2	2.0
Genomic	LMHCops	Live cone	60 $\pm$ 9	28	3	-
Genomic	LMHCops	Fixed cone	30 $\pm$ 3	25	3	2.1
Somatic (AAV2/5)	CMV	Fixed cone	40 $\pm$ 10	11	4	
Somatic (AAV2/5)	CMV	Fixed RPE cell	680 $\pm$ 170	12	1	
Somatic (AAV2/5)	CMV	Fixed Müller cell	150 $\pm$ 90	3	1	
Somatic (AAV2/5)	CMV	Fixed amacrine	65 $\pm$ 10	11	1	
Somatic (AAV2/5)	CMV	Fixed ganglion	45 $\pm$ 5	12	1	
Somatic (AAV2/2)	CMV	Fixed cone	15 $\pm$ 3	2		
Somatic (AAV2/2)	CMV	Fixed RPE cell	300 $\pm$ 110	6		
Somatic (AAV2/2)	CMV	Fixed Müller cell	20	1		
Somatic (AAV2/2)	CMV	Fixed amacrine	45 $\pm$ 5	8		
Somatic (AAV2/2)	CMV	Fixed ganglion	62 $\pm$ 10	7		

Column 1 specifies the means by which the enhanced green fluorescent protein cDNA was delivered. Genomic delivery was accomplished through microinjection of zygote pronuclei; column 2 lists the promoter; column 3 gives the cell type. Column 4 gives the estimated EGFP concentration (Figure 2); the values are mean $\pm$ SEM, with the average taken over the number of cells indicated in column 5. Column 6 shows the numbers of retinas analyzed. The final column provides ratios of estimated expression levels for fixed compared to non-fixed cells (column 7).

previously [18], EGFP is present exclusively in cones, whose morphology is beautifully revealed (Figure 1C; see also Figure 2). The retinas of these pLMCops.EGFP mice, like those of the p $\beta$ Act.EGFP mice, appear completely normal in the light microscope, with normal layer thickness, normal cone density and matrix labeling by PNA (Figure 1C,D).

*EGFP levels reach several hundred micromolar in many retinal cell types in utero:* We determined the exact levels of EGFP in different cells of live mouse neural retinas (Figure 3) with published methods [22]. EGFP is a highly soluble protein [26], and its fluorescence intensity in live cells correlates with the local cytoplasmic volume fraction of different sub-cellular regions [22]. In rod cells, the most intense fluorescence is found in the myoid region of the inner segment, located between the nucleus and the ellipsoid, and in the perinuclear region (Figure 3A; see also Figure 1A). In cone cells, whose images are readily excised from the 3D confocal laser scanning microscope (CLSM) scan matrix of retinal slices of the pLMCops.EGFP mouse, the most intensely fluorescent regions are likewise in the inner segment and perinuclear region, but also include the cone synaptic pedicle (Figure 3B; see also Figure 2). The absolute concentration of EGFP in each 3D volume element or “voxel” was estimated from the images of the live rods and cones with published methods: the

average level of the voxels whose intensities were in the upper 10<sup>th</sup> percentile of the histograms (Figure 3C,D) were taken as the true concentration in the cell cytoplasm [22]. In addition to rods and cones, the same analysis was applied to several other readily identified retinal cell types of p $\beta$ Act.EGFP and pLMCops.EGFP mice; the results are summarized in Table 1 (see also Figure 4, Figure 5, and Figure 6).

EGFP concentrations were also estimated in retinal cells of mice transduced with either one of two serotypes of AAV

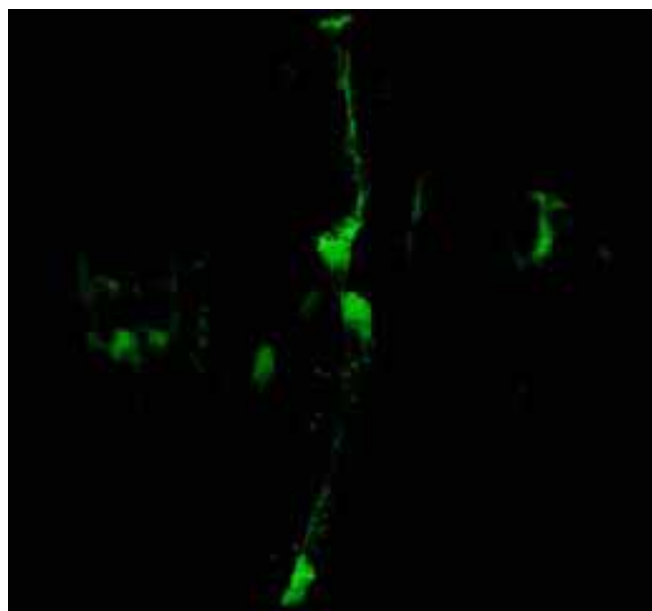


Figure 5. Morphology of a Müller cell from an AAV2/5.CMV.EGFP-infected retina. Three-dimensional confocal images showing distribution of enhanced green fluorescent protein in a Müller cell. One Müller cell is seen to span the entire width of the retina in this image and portions of others are apparent as well. For the cell which spans the entire retina, the endfoot (vitreal aspect of the cell) is oriented toward the top of the image and the portion of the cell adjacent to photoreceptors is at the bottom of the image. Müller cell nuclei appear as rounded structures approximately mid-way across the retina. Processes project from the main trunks of the Müller cells. A quicktime movie of this figure is available in the online version of this article. A representative frame is included here.

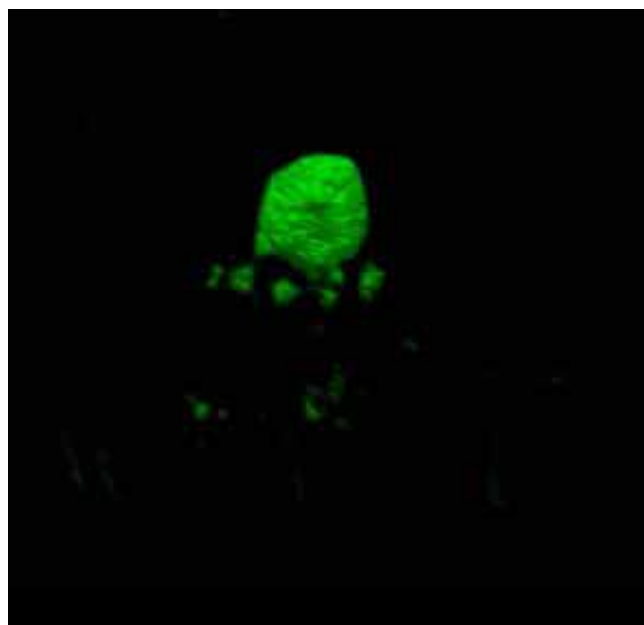


Figure 4. Morphology of an amacrine cell from an AAV2/5.CMV.EGFP-infected retina. Three-dimensional representation of a z-stack of confocal images from an AAV2/5.CMV.EGFP infected mouse retina showing the distribution of enhanced green fluorescent protein in a representative amacrine cell. A quicktime movie of this figure is available in the online version of this article. A representative frame is included here.

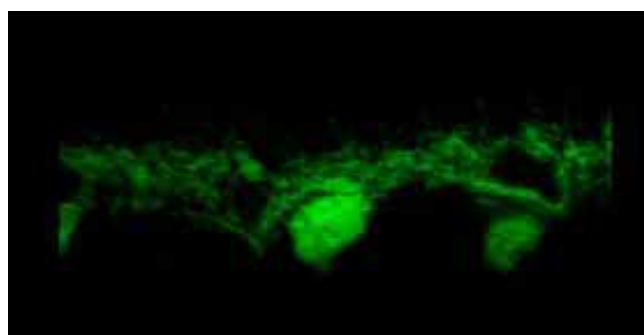


Figure 6. Morphology of a horizontal cell from an AAV2/5.CMV.EGFP-infected retina. Three-dimensional representation of a z-stack of confocal images from an AAV2/5.CMV.EGFP infected mouse retina showing the distribution of enhanced green fluorescent protein in a representative horizontal cell. A quicktime movie of this figure is available in the online version of this article. A representative frame is included here.

(AAV2/5.CMV.EGFP; AAV2/2.CMV.EGFP). These viruses had been used to deliver the *EGFP* cDNA with a CMV promoter to the subretinal space by injection in utero (Table 1). As previously described, such infection drives expression in sets of progenitor cells and their progeny across a wide region of the retina. Injections of AAV2/5 at E14 result in high levels of transgene expression in cells destined to become cone photoreceptors and RPE cells and lesser levels in certain inner retinal cells [4].

For some experiments, we employed frozen sections of the whole retina rather than live tissue for analysis. By fixing tissue on the stage of the CLSM, we found that the fixation itself decreased EGFP fluorescence by approximately 2 fold (Table 1, compare rows identified as “live” and “fixed” cells of the same type). Thus, we suggest that all EGFP protein levels for fixed tissue be adjusted upward 2 fold to correct for this fixation effect (no corrections have been applied to the data in Table 1, however).

Scrutiny of the summary data in Table 1 reveals that EGFP protein levels for the different promoters and transgene delivery methods range from 30  $\mu\text{M}$  to about 700  $\mu\text{M}$ . It is notable that AAV2/5 infection with the *EGFP* cDNA driven by the CMV promoter achieves EGFP protein levels exceeding those seen in cells of transgenic mice in which expression is driven by the constitutively active  $\beta$ -actin promoter. The RPE cells of AAV2/5-transduced mice, when corrected for the fixation artifact, are estimated to have nearly 1.4 mM EGFP (Table 1). Another quantitative feature of the data is that gene transfer with AAV2/2 results in EGFP protein levels on average approximately 2 fold less than AAV2/5.

*High levels of EGFP do not interfere with retinal function:* The potential toxicity of EGFP is an issue of concern to researchers using the protein as a reporter to investigate transgene delivery and promoter efficiency in the retina [11-17,27]. Retinal rods are of particular interest in this regard, as they outnumber all other retinal cells by 20 to 1 [28], and when

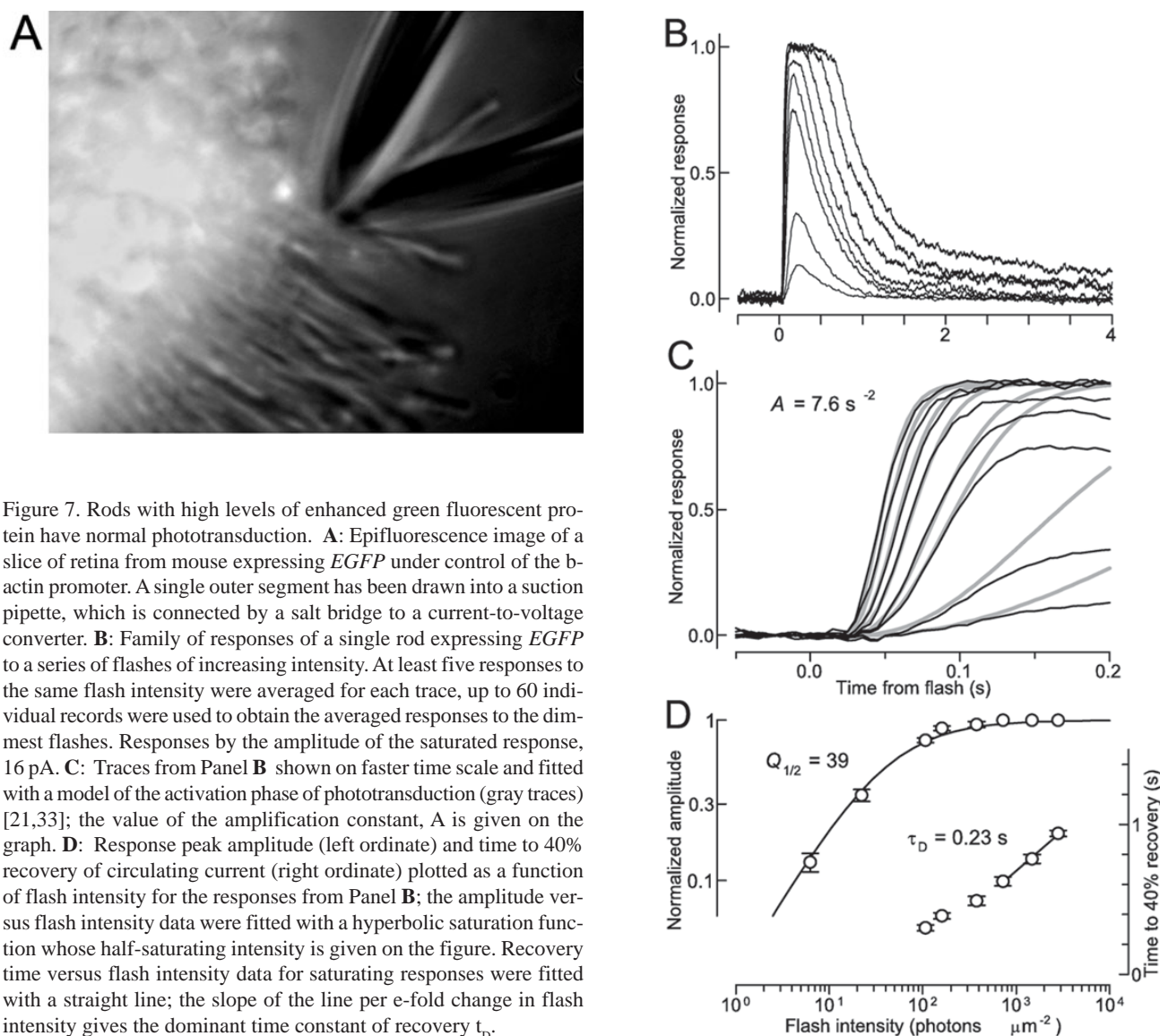


Figure 7. Rods with high levels of enhanced green fluorescent protein have normal phototransduction. **A:** Epifluorescence image of a slice of retina from mouse expressing *EGFP* under control of the  $\beta$ -actin promoter. A single outer segment has been drawn into a suction pipette, which is connected by a salt bridge to a current-to-voltage converter. **B:** Family of responses of a single rod expressing *EGFP* to a series of flashes of increasing intensity. At least five responses to the same flash intensity were averaged for each trace, up to 60 individual records were used to obtain the averaged responses to the dimmest flashes. Responses by the amplitude of the saturated response, 16 pA. **C:** Traces from Panel **B** shown on faster time scale and fitted with a model of the activation phase of phototransduction (gray traces) [21,33]; the value of the amplification constant,  $A$  is given on the graph. **D:** Response peak amplitude (left ordinate) and time to 40% recovery of circulating current (right ordinate) plotted as a function of flash intensity for the responses from Panel **B**; the amplitude versus flash intensity data were fitted with a hyperbolic saturation function whose half-saturating intensity is given on the figure. Recovery time versus flash intensity data for saturating responses were fitted with a straight line; the slope of the line per e-fold change in flash intensity gives the dominant time constant of recovery  $t_D$ .

dysfunctional, cause collateral damage in other cells [29]. To assess the function of rods expressing EGFP we measured the electrical responses of single rods with suction pipette methods (Figure 7). Such recordings from rods of pβAct.EGFP mice revealed these cells response properties to be statistically indistinguishable from those of rods of WT (i.e., non-transgenic) mice (Figure 7A,B, Table 2).

To assess other aspects of retinal function we employed full-field, single-flash electroretinograms (ERGs; Table 3, Figure 8): such recordings allow assessment of the electrical responses of a number of cell types, including those of rod bipolar cells (scotopic b-waves, Table 3, Figure 8A), rods (dark adapted a-waves, Table 3, Figure 8B) and cone on-bipolars (photopic b-waves, Table 3, Figure 8C). The properties of the components of the ERG responses of the pβAct.EGFP and AAV2/2 or AAV2/5-injected mice are statistically indistin-

guishable from those of WT mice (Table 3) [4]. There do appear to be differences in the ERG responses of the pLMCOps mice as compared to WT, in that the  $a_{max}$  and cone  $b_{max}$  values are lower in the pLMCOps mice (Table 3).

### DISCUSSION

*High levels of EGFP in retinal cells are not deleterious to retinal cells:* Green fluorescent protein-and in particular the variant known as enhanced green fluorescent protein (EGFP)-has become an extremely useful reagent in cell biology [23,24]. This utility arises from the intrinsic properties of EGFP, including its large optical cross section ( $\epsilon_{max}=58,000$ ), high quantum efficiency for fluorescence ( $\gamma=0.75$ ) and very high solubility [17,19,24], and also from its ability to be added genetically as a tag to proteins to track their location and movements [25-28]. Finally, and of direct relevance to this study,

**TABLE 2. ELECTROPHYSIOLOGICAL PROPERTIES OF SINGLE WT RODS AND RODS EXPRESSING EGFP UNDER CONTROL OF THE B-ACTIN PROMOTER**

Genotype (number)	rmax	SF	A	tpeak	tD
pβ-actin-EGFP (11)	20±12	0.05±0.01	7.2±1.0	210±10	250±20
WT (10)	15± 4	0.05±0.01	8.0±1.6	220±10	210±40

The first column identifies the genotype of the animal from which the retinal slice was taken and recordings from individual rod outer segments were made (Figure 3); the number in parentheses gives the number of rods recorded. The other columns give the parameters of phototransduction measured from the rod responses: rmax is the amplitude of the saturated photocurrent response in pA; SF is the dim-flash sensitivity, expressed as the fraction of the maximum current [ $\Delta R = \Delta r(t_{peak})/r_{max}$ ] suppressed per photoisomerization; A is the amplification coefficient in  $s^{-2}$  (Figure 3C); tpeak is the time to peak of the dim-flash response in ms; tD is the dominant recovery time constant of just-saturating flashes in ms (Figure 3D). A collecting area of 0.5 mm<sup>2</sup> was assumed for all rods [33]. All entries are means±95% confidence intervals, and none of the parameters were reliably different between rods of the two genotypes.

**TABLE 3. PROPERTIES OF ELECTRORETINOGRAMS OF MICE WITH GENOMIC DELIVERY OF ENHANCED GREEN FLUORESCENT PROTEIN**

Promoter	Age (weeks)	bmax (rods; μV)	Sb ( $\Delta\beta/\Phi$ )	amax (μV)	A	bmax (cones; μV)
β-actin	8	120	0.24	200	2.6	100
β-actin	5	350	0.48	365	2.0	225
β-actin	5	470	0.13	420	3.3	200
β-actin	5	550	0.16	370	7.5	200
LMHCops	7	140	0.25	225	2.8	60
LMHCops	7	245	ND	320	ND	75
LMHCops	7	370	0.24	400	8.0	86
LMHCops	7	410	0.14	390	9.8	95
LMHCops	7	475	0.22	323	3.6	65
WT controls*	8	415±140	0.28±0.04	550±125	7.4±2.5	210±55

(Mean±SD; n=56)

Column 1 identifies the promoter driving enhanced green fluorescent protein expression in an individual transgenic animal. All animals were between six and eight weeks of age at the time of electroretinogram (ERG) testing. Columns 2-6 of the first row identify specific parameters measured from the ERG (see Figure 4): bmax (rods), the saturating amplitude of the scotopic b-wave (Figure 4A); Sb represents the sensitivity of the scotopic b-wave expressed as fraction of the normalized response per photoisomerization; amax is the saturating amplitude of the a-wave and A is the amplification coefficient (with dimensions  $s^{-2}$ ), estimated from a set of a-waves (Figure 4B); bmax (cones) is the saturating amplitude of the cone-driven b-wave. "ND" signifies "not determined." The final row of the table gives average parameters from a population of C57Bl/6 mice of 8 wks age [34] (Table 2). Asterisk indicates that the ERG experiments in [34] were performed with the reference electrode inserted into the animals forehead, while for those reported here the reference electrode was in the mouth. The amplitudes for bmax and amax of the WT population data have been multiplied by the experimentally determined scale factor 1.9 to account for the change in reference electrode placement.

EGFP can be precisely quantified in living cells [22]. Nonetheless, for these useful features to be useful in the context of experiments aimed at understanding and improving exogenous gene transfer, it is critical to assess the potential of EGFP for deleterious effects on cell function. As such effects can be expected to depend on the concentration, we undertook to quantify EGFP protein present in various cells after delivery of *EGFP*. We studied a variety of different situations, including those where *EGFP* is present in different copy numbers, where the *EGFP* cassette is integrated in the genome (in transgenic mice) versus predominantly episomal (after virus delivery) and where *EGFP* is driven by different promoters.

EGFP at concentrations up to several hundred micromolar is clearly not deleterious to retinal cell health. Photoreceptors containing 270  $\mu\text{M}$  EGFP have normal morphology (Figure 1, Figure 3) [4] and completely normal electrical responses (Figure 7, Figure 8, Table 3) [4]. It is thus clear from these measurements that 270  $\mu\text{M}$  EGFP (Figure 3, Table 1), does not interfere in any way with the amplification of the phototransduction process (Figure 7, Figure 8, Table 2, Table 3), nor with the highly active molecular processes in the inner segment that synthesize and deliver phototransduction proteins to the outer segment.

Other retinal cells possessing high levels of EGFP have normal morphology as reported here (Figure 1, Figure 3), and in previous studies [4,30]. The only apparent exception to this rule is one study using lentivirus to express *EGFP* in rabbit RPE [27]. In that study, it may have been an immune response, not EGFP levels per se, that resulted in toxicity. In the present study, there is a suggestion of diminished cone function in cone in LMHCops.EGFP mice. In these animals, the amplitudes of the cone-driven b-waves are reduced to about half the values in the other mice, including WT mice (Table 3). This could potentially indicate toxicity of EGFP in cone photoreceptors. However, much lower levels of EGFP were measured in cones of LMCops.EGFP animals than in the cones of mice that received the transgene in other ways (Table 1, Table 3) [4]. Thus, presence of EGFP per se is not toxic to these cells. There were no indications from histology of retinal degeneration in these animals (data not shown). Nonetheless, it is possible that there are changes in numbers of cone photoreceptors that have not yet been appreciated. Other explanations remain possible for the reduction of the b-wave. For example, the transgene in the pLMCops.EGFP mice may have inserted in a location that alters regulation of a second cone-specific gene.

*EGFP fluorescence is diminished in fixed tissue:* Confocal scanning of live and fixed retinas of p $\beta$ Act.EGFP mice led us to suspect that the fixation process lowered the fluorescence of EGFP. We confirmed this suspicion by scanning the same slice of retina before, during and after fixation, and found on average a reduction of fluorescence of about 2 fold (Table 1). Others have previously reported such effects [31,32]. In experiments with *Xenopus* rods (data not shown) we found the effect could be as great as a 10 fold decrease in fluorescence in the large *Xenopus* rod outer segment. We suggest that the cross-linking that occurs during fixation disrupts the

EGFP chromophore, but may do so in a manner that depends on the local protein and lipid environment. Thus, in the outer segment, the high density of native protein (the concentration of rhodopsin is about 6 mM relative to the outer segment water space) may contribute to the effect. Such fixation artifacts

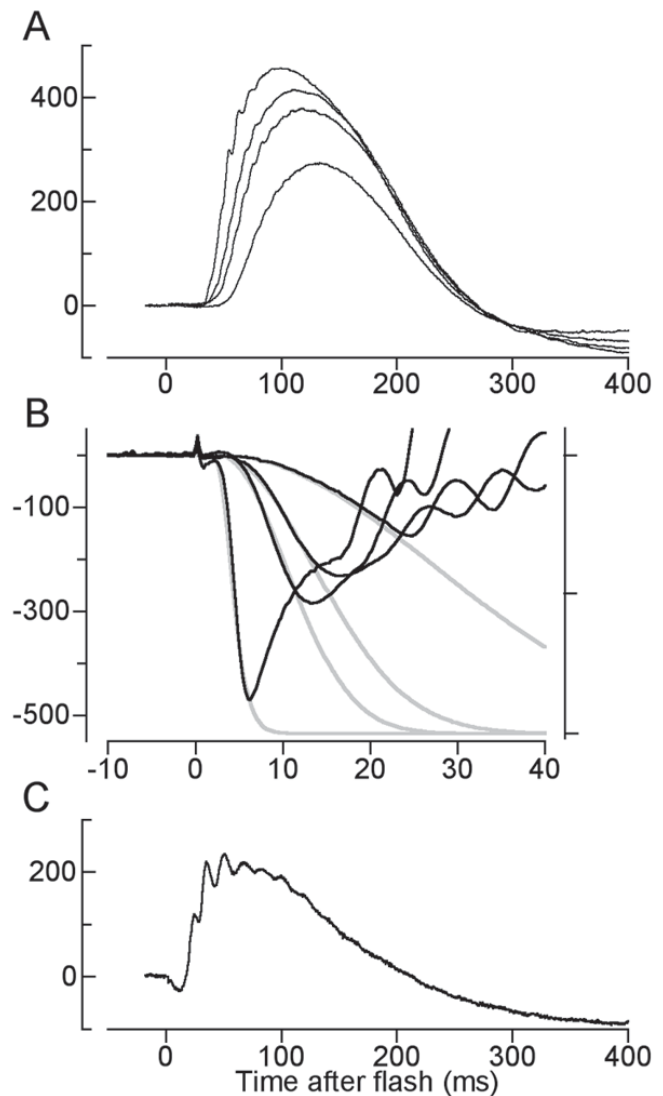


Figure 8. Electrophysiological recordings from a mouse expressing *EGFP* under control of the b-actin promoter. **A:** Scotopic b-waves are responses to Ganzfeld flashes of luminance  $3 \times 10^{-4}$ ,  $8.6 \times 10^{-3}$ , and  $3.2 \times 10^{-3}$  scotopic  $\text{cd s m}^{-2}$ . **B:** Rod a-waves are responses to flashes of 0.7, 3.7, 7.5, and 206 scotopic  $\text{cd s m}^{-2}$ . The traces are shown on a ten fold faster time base than those in A; the saturating amplitude, obtained in response to the most intense flash is 471 mV. The normalized traces (right ordinate) have been fitted with a model of the rod phototransduction cascade [33]. Assuming a dilated pupil area of  $3.2 \text{ mm}^2$  and conversion factor for scot Td s to photoisomerizations of 171 [34], the amplification coefficient obtained from the fitting is  $A=4.4 \text{ s}^{-2}$ . **C:** Photopic b-wave are the same intensity flash as was used to produce the saturating a-wave in B was presented in the presence of a steady background that suppressed rod activity (as evidenced by the absence of all but a small a-wave, which is attributable to cones). The cone-driven b-wave amplitude (with oscillations filtered out) is 200 mV.

need to be taken into consideration in experiments in which fixed tissue is used to assess levels of EGFP.

*EGFP can be used to quantitatively assess the efficiency of different gene delivery methods:* Our results show that EGFP can be used to quantitatively assess the relative efficiency of different methods of delivering transgenes (Table 1). EGFP levels were approximately 2 fold higher in most cell types transduced with AAV2/5.CMV.EGFP as compared with those transduced with AAV2/2.CMV.EGFP. Previous studies provided qualitative data describing more efficient transduction mediated by AAV2/5 as compared to AAV2/2 [4,6,16,17]. Results from the present study provide quantitative confirmation.

The highest observed level of EGFP fluorescence was in RPE cells. Indeed, after correcting for the fixation effect (multiplying by 2), we estimated the EGFP concentration to be nearly 1.4 mM in the RPE. One possible explanation for the higher efficacy of virus-mediated gene transfer to RPE cells relative to photoreceptors is the relative surface areas of the membranes facing the subretinal space. Thus, the convoluted apical surfaces of RPE cells likely present a larger surface area that can be bound by viruses delivered to the subretinal space than does the outer segment membrane of photoreceptors. RPE cells can also phagocytize materials from other cells (i.e., EGFP-positive outer segments), and this may also result in enhanced EGFP levels in these cells.

*Conclusion:* This study compares, in individual cell types of the retina, the amount of a protein produced as a result of standard (genomic) transgenic methods compared to virus-mediated gene transfer. The data reveal that transgenesis effected by different methods can be quantitatively compared. Given the clearly low level of toxicity of EGFP, these data provide a foundation for the quantitation of delivery of EGFP-fusion proteins that may serve therapeutic purposes.

#### ACKNOWLEDGEMENTS

This study was supported by R01 EY10820, EY12156 (JB), EY02660 (EP), 5-P30-DK-47747-10 (Vector Core Facility), the Foundation Fighting Blindness, the Lew R. Wasserman Award from Research to Prevent Blindness, the Paul and Evanina Mackall Trust, and the F. M. Kirby Foundation. We thank K. Maguire for technical advice.

#### REFERENCES

- Allegra S, Bouazza L, Benetollo C, Li JY, Langlois D. A 7.1 kbp beta-myosin heavy chain promoter, efficient for green fluorescent protein expression, probably induces lethality when overexpressing a mutated transforming growth factor-beta type II receptor in transgenic mice. *Transgenic Res* 2005; 14:69-80.
- Dominici M, Tadjali M, Kepes S, Allay ER, Boyd K, Ney PA, Horwitz E, Persons DA. Transgenic mice with pancellular enhanced green fluorescent protein expression in primitive hematopoietic cells and all blood cell progeny. *Genesis* 2005; 42:17-22.
- Ahmed BY, Chakravarthy S, Eggers R, Hermens WT, Zhang JY, Niclou SP, Levelt C, Sablitzky F, Anderson PN, Lieberman AR, Verhaagen J. Efficient delivery of Cre-recombinase to neurons in vivo and stable transduction of neurons using adeno-associated and lentiviral vectors. *BMC Neurosci* 2004; 5:4.
- Surace EM, Auricchio A, Reich SJ, Rex T, Glover E, Pineles S, Tang W, O'Connor E, Lyubarsky A, Savchenko A, Pugh EN Jr, Maguire AM, Wilson JM, Bennett J. Delivery of adeno-associated virus vectors to the fetal retina: impact of viral capsid proteins on retinal neuronal progenitor transduction. *J Virol* 2003; 77:7957-63.
- Guo TQ, Wang JY, Guo XY, Wang SP, Lu CD. Transient in vivo gene delivery to the silkworm *Bombyx mori* by EGT-null recombinant AcNPV using EGFP as a reporter. *Arch Virol* 2005; 150:93-105.
- Auricchio A, Kobinger G, Anand V, Hildinger M, O'Connor E, Maguire AM, Wilson JM, Bennett J. Exchange of surface proteins impacts on viral vector cellular specificity and transduction characteristics: the retina as a model. *Hum Mol Genet* 2001; 10:3075-81.
- Acland GM, Aguirre GD, Ray J, Zhang Q, Aleman TS, Cideciyan AV, Pearce-Kelling SE, Anand V, Zeng Y, Maguire AM, Jacobson SG, Hauswirth WW, Bennett J. Gene therapy restores vision in a canine model of childhood blindness. *Nat Genet* 2001; 28:92-5.
- Acland GM, Aguirre GD, Bennett J, Aleman TS, Cideciyan AV, Bencicelli J, Dejneka NS, Pearce-Kelling SE, Maguire AM, Palczewski K, Hauswirth WW, Jacobson SG. Long-Term Restoration of Rod and Cone Vision by Single Dose rAAV-Mediated Gene Transfer to the Retina in a Canine Model of Childhood Blindness. *Mol Ther* 2005; 12:1072-82.
- Dejneka NS, Surace EM, Aleman TS, Cideciyan AV, Lyubarsky A, Savchenko A, Redmond TM, Tang W, Wei Z, Rex TS, Glover E, Maguire AM, Pugh EN Jr, Jacobson SG, Bennett J. In utero gene therapy rescues vision in a murine model of congenital blindness. *Mol Ther* 2004; 9:182-8.
- Narfstrom K, Katz ML, Bragadottir R, Seeliger M, Boulanger A, Redmond TM, Caro L, Lai CM, Rakoczy PE. Functional and structural recovery of the retina after gene therapy in the RPE65 null mutation dog. *Invest Ophthalmol Vis Sci* 2003; 44:1663-72.
- Daniels DM, Shen WY, Constable IJ, Rakoczy PE. Quantitative model demonstrating that recombinant adeno-associated virus and green fluorescent protein are non-toxic to the rat retina. *Clin Experiment Ophthalmol* 2003; 31:439-44.
- Bennett J, Maguire AM, Cideciyan AV, Schnell M, Glover E, Anand V, Aleman TS, Chirmule N, Gupta AR, Huang Y, Gao GP, Nyberg WC, Tazelaar J, Hughes J, Wilson JM, Jacobson SG. Stable transgene expression in rod photoreceptors after recombinant adeno-associated virus-mediated gene transfer to monkey retina. *Proc Natl Acad Sci U S A* 1999; 96:9920-5.
- Bennett J, Anand V, Acland GM, Maguire AM. Cross-species comparison of in vivo reporter gene expression after recombinant adeno-associated virus-mediated retinal transduction. *Methods Enzymol* 2000; 316:777-89.
- Nour M, Quiambao AB, Al-Ubaidi MR, Naash MI. Absence of functional and structural abnormalities associated with expression of EGFP in the retina. *Invest Ophthalmol Vis Sci* 2004; 45:15-22.
- Le Meur G, Weber M, Pereon Y, Mendes-Madeira A, Nivard D, Deschamps JY, Moullier P, Rolling F. Postsurgical assessment and long-term safety of recombinant adeno-associated virus-mediated gene transfer into the retinas of dogs and primates. *Arch Ophthalmol* 2005; 123:500-6.
- Yang GS, Schmidt M, Yan Z, Lindbloom JD, Harding TC, Donahue BA, Engelhardt JF, Kotin R, Davidson BL. Virus-mediated transduction of murine retina with adeno-associated

- virus: effects of viral capsid and genome size. *J Virol* 2002; 76:7651-60.
17. Rabinowitz JE, Rolling F, Li C, Conrath H, Xiao W, Xiao X, Samulski RJ. Cross-packaging of a single adeno-associated virus (AAV) type 2 vector genome into multiple AAV serotypes enables transduction with broad specificity. *J Virol* 2002; 76:791-801.
  18. Fei Y, Hughes TE. Transgenic expression of the jellyfish green fluorescent protein in the cone photoreceptors of the mouse. *Vis Neurosci* 2001; 18:615-23.
  19. Lyubarsky AL, Pugh EN Jr. Recovery phase of the murine rod photoresponse reconstructed from electroretinographic recordings. *J Neurosci* 1996; 16:563-71.
  20. Lyubarsky AL, Falsini B, Pennesi ME, Valentini P, Pugh EN Jr. UV- and midwave-sensitive cone-driven retinal responses of the mouse: a possible phenotype for coexpression of cone photopigments. *J Neurosci* 1999; 19:442-55.
  21. Nikonov SS, Daniele LL, Zhu X, Craft CM, Swaroop A, Pugh EN Jr. Photoreceptors of *Nrl*  $-/-$  mice coexpress functional S- and M-cone opsins having distinct inactivation mechanisms. *J Gen Physiol* 2005; 125:287-304.
  22. Peet JA, Bragin A, Calvert PD, Nikonov SS, Mani S, Zhao X, Besharse JC, Pierce EA, Knox BE, Pugh EN Jr. Quantification of the cytoplasmic spaces of living cells with EGFP reveals arrestin-EGFP to be in disequilibrium in dark adapted rod photoreceptors. *J Cell Sci* 2004; 117:3049-59.
  23. Okabe M, Ikawa M, Kominami K, Nakanishi T, Nishimune Y. 'Green mice' as a source of ubiquitous green cells. *FEBS Lett* 1997; 407:313-9.
  24. Dudus L, Anand V, Acland GM, Chen SJ, Wilson JM, Fisher KJ, Maguire AM, Bennett J. Persistent transgene product in retina, optic nerve and brain after intraocular injection of rAAV. *Vision Res* 1999; 39:2545-53.
  25. Blanks JC, Johnson LV. Specific binding of peanut lectin to a class of retinal photoreceptor cells. A species comparison. *Invest Ophthalmol Vis Sci* 1984; 25:546-57.
  26. Luby-Phelps K. Cytoarchitecture and physical properties of cytoplasm: volume, viscosity, diffusion, intracellular surface area. *Int Rev Cytol* 2000; 192:189-221.
  27. Doi K, Hargitai J, Kong J, Tsang SH, Wheatley M, Chang S, Goff S, Gouras P. Lentiviral transduction of green fluorescent protein in retinal epithelium: evidence of rejection. *Vision Res* 2002; 42:551-8.
  28. Jeon CJ, Strettoi E, Masland RH. The major cell populations of the mouse retina. *J Neurosci* 1998; 18:8936-46.
  29. Hicks D, Sahel J. The implications of rod-dependent cone survival for basic and clinical research. *Invest Ophthalmol Vis Sci* 1999; 40:3071-4.
  30. Kuzmanovic M, Dudley VJ, Sarthy VP. GFAP promoter drives Muller cell-specific expression in transgenic mice. *Invest Ophthalmol Vis Sci* 2003; 44:3606-13.
  31. Brock R, Hamelers IH, Jovin TM. Comparison of fixation protocols for adherent cultured cells applied to a GFP fusion protein of the epidermal growth factor receptor. *Cytometry* 1999; 35:353-62.
  32. Schmitz HD, Bereiter-Hahn J. GFP associates with microfilaments in fixed cells. *Histochem Cell Biol* 2001; 116:89-94.
  33. Lamb TD, Pugh EN Jr. A quantitative account of the activation steps involved in phototransduction in amphibian photoreceptors. *J Physiol* 1992; 449:719-58.
  34. Lyubarsky AL, Daniele LL, Pugh EN Jr. From candelas to photoisomerizations in the mouse eye by rhodopsin bleaching in situ and the light-rearing dependence of the major components of the mouse ERG. *Vision Res* 2004; 44:3235-51.